Structural basis of Vps33A recruitment to the human HOPS complex by Vps16

Stephen C. Graham[a,b,1,2], Lena Wartosch[a,1], Sally R. Gray[a], Edward J. Scourfield[b], Janet E. Deane[c], J. Paul Luzio[a,2], and David J. Owen[a]

Departments of [a]Clinical Biochemistry and [c]Haematology, Cambridge Institute for Medical Research, University of Cambridge, Cambridge CB2 0XY, United Kingdom; and [b]Department of Pathology, University of Cambridge, Cambridge CB2 1QP, United Kingdom

Edited by William T. Wickner, Dartmouth Medical School, Hanover, NH, and approved July 8, 2013 (received for review April 15, 2013)

The multisubunit homotypic fusion and vacuole protein sorting (HOPS) membrane-tethering complex is required for late endosome-lysosome and autophagosome-lysosome fusion in mammals. We have determined the crystal structure of the human HOPS subunit Vps33A, confirming its identity as a Sec1/Munc18 family member. We show that HOPS subunit Vps16 recruits Vps33A to the human HOPS complex and that residues 642–736 are necessary and sufficient for this interaction, and we present the crystal structure of Vps33A in complex with Vps16(642–736). Mutations at the binding interface disrupt the Vps33A–Vps16 interaction both in vitro and in cells, preventing recruitment of Vps33A to the HOPS complex. The Vps33A–Vps16 complex provides a structural framework for studying the association between Sec1/Munc18 proteins and tethering complexes.

Eukaryotic cells tightly regulate the movement of macromolecules between their membrane-bound compartments. Multiple proteins and protein complexes interact to identify vesicles or organelles destined to fuse, bring them into close proximity, and then fuse their membranes, thereby allowing their contents to mix (1). Multisubunit tethering complexes modulate key steps in these fusion events by recognizing specific Rab-family small GTPases on the membrane surfaces, physically docking the membranes and then recruiting the machinery that effects the membrane fusion (2, 3).

In metazoans, the multisubunit tethering complex homologous to the yeast homotypic fusion and vacuole protein sorting (HOPS) complex (4–7) is required for the maturation of endosomes (8); the delivery of cargo to lysosomes (9) and lysosome-related organelles, such as pigment granules in *Drosophila melanogaster* (10); and the fusion of autophagosomes with late endosomes/lysosomes (11). The mammalian HOPS complex comprises six subunits (Vps11, Vps16, Vps18, Vps33A, Vps39, and Vps41) (4–6). Homologs of HOPS components can be identified in almost all eukaryotic genomes (12) and are thought to be essential; for example, removal of the Vps33A homolog *carnation* (*car*) in *Drosophila* is lethal during larval development (13).

HOPS components have been identified in animal models of human disease. A missense point mutation in the murine *Vps33a* gene gives rise to the *buff* mouse phenotype, characterized by pigmentation, platelet activity, and motor deficiencies (14). This phenotype closely resembles the clinical presentation of Hermansky–Pudlak syndrome (HPS) (15), and a mutation in the human *VPS33A* gene has been observed in a patient with HPS who lacked mutations at other known HPS loci (14). In metazoans, there is a second homolog of yeast Vps33 called Vps33B, but disruption of the *VPS33B* gene in humans gives rise to a clinical phenotype distinct from HPS (16).

Human Vps33A is predicted to be a member of the Sec1/Munc18 (SM) family of proteins (7, 17) that, together with SNAREs, comprise the core machinery essential for membrane fusion in eukaryotes (18). Three SNAREs with glutamine residues at the center of their SNARE domain (Q_a-, Q_b-, and Q_c-SNAREs) and one with a central arginine residue (R-SNARE) associate to form a four-helical bundle, the trans-SNARE complex. Formation of this trans-SNARE complex by SNAREs on adjacent membranes drives the fusion of these membranes (18). SM proteins are essential regulators of this process, promoting membrane fusion by correctly formed (cognate) SNARE complexes (18). Although a comprehensive understanding of how SM proteins achieve this still remains elusive, it is clear that SM proteins bind directly both to individual SNAREs and to SNARE complexes (18, 19). Most SM proteins bind strongly and specifically to an N-terminal segment of their cognate Q_a-SNARE, the N-peptide, and this interaction is thought to recruit the SM protein to the site of SNARE-mediated fusion (20, 21).

When considered as a whole, the HOPS complex has the functional characteristics of an SM protein: It binds SNAREs and SNARE complexes (5, 22–24), and yeast HOPS has been shown to promote SNARE-mediated membrane fusion (25, 26). Recent biochemical analysis of Vps33, the yeast Vps33A homolog, shows it to be capable of binding isolated SNARE domains and SNARE complexes but not the N-terminal domain or full cytosolic portion of the Q_a-SNARE Vam3 (23, 24). Data from the yeast HOPS complex are consistent with a model whereby Vps33 provides the SM functionality of HOPS, accelerating SNARE-mediated fusion, whereas the rest of the HOPS complex recruits Vps33 (and thus SM function) to the site of SNARE-mediated fusion (24).

Although a recent EM study has defined the overall topology of the yeast HOPS complex (27), atomic resolution insights into the assembly of the HOPS complex have thus far been unavailable. Here, we present the 2.4-Å resolution structure of human Vps33A, confirming its structural identity as an SM protein. We have mapped the HOPS epitope that binds Vps33A to a helical fragment comprising residues 642–736 of Vps16, solved the structure of this complex to 2.6-Å resolution, and identified mutations at the binding interface that disrupt the Vps33A–Vps16 complex both in vitro and in cultured cells.

Results

Structure of Vps33A Confirms It to Have an SM-Like Fold. Human Vps33A was expressed in *Escherichia coli*, purified, crystallized, and its structure was solved by single isomorphous replacement with anomalous scattering using a lead derivative. Two molecules of Vps33A are present in the asymmetrical unit, with continuous electron density being present for the entire mature protein (residues 2–596) except for the loops connecting residues 326–336, 530–543, and 269–280 (with the latter being absent in only one of the two Vps33A molecules in the asymmetrical unit). The

Author contributions: S.C.G., L.W., J.P.L., and D.J.O. designed research; S.C.G., L.W., S.R.G., and E.J.S. performed research; J.E.D. contributed new reagents/analytic tools; S.C.G., L.W., J.E.D., J.P.L., and D.J.O. analyzed data; and S.C.G., L.W., J.P.L., and D.J.O. wrote the paper.

The authors declare no conflict of interest.

This article is a PNAS Direct Submission.

Freely available online through the PNAS open access option.

Data deposition: The atomic coordinates and structure factors have been deposited in the Protein Data Bank, www.pdb.org [PDB ID codes 4bx8 (Vps33A) and 4bx9 (Vps33A–Vps16)].

[1]S.C.G. and L.W. contributed equally to this work.

[2]To whom correspondence may be addressed. E-mail: scg34@cam.ac.uk or jpl10@cam.ac.uk.

This article contains supporting information online at www.pnas.org/lookup/suppl/doi:10.1073/pnas.1307074110/-/DCSupplemental.

final structure was refined to a resolution of 2.4 Å with residuals R = 0.197 and R_{free}= 0.244 and with excellent stereochemistry, with 98% of residues occupying the most favored region of the Ramachandran plot (Table S1).

Vps33A adopts an SM fold (Fig. 1), despite sharing less than 20% sequence identity with previously characterized SM proteins. As observed for other SM proteins (28), a flexible hinge connects the N-terminal domain 1 to the C-terminal domains 2 and 3, with the orientation of domain 1 relative to domains 2 and 3 differing by 3.1° between the two Vps33A molecules in the asymmetrical unit. Domains 1 and 2 are well conserved across all SM protein structures, as are the core helices of domains 3a and 3b that pack against domain 2 and the long kinked helix that links domains 3a and 3b. The remainder of domains 3a and 3b, including the residues that contact the SNARE H_{abc} domain (29, 30), comprises similar secondary structural elements across SM proteins, but their orientations differ relative to those of the core helices. Structure-based phylogenetic analysis shows the SM proteins that function at the plasma membrane to be more similar to each other than they are to SM proteins that function on endomembranes, such as Vps33A (Fig. S1).

Superposition of Vps33A on the *Monosiga brevicollis* UNC18–syntaxin 1 complex reveals that, as suggested previously (31), Vps33A lacks a pocket for binding a typical Q_a-SNARE N-terminal peptide (Fig. 1). Structural mapping of the single amino acid mutations that give rise to the *Drosophila car* and mouse *buff* phenotypes, as well as of the mutation of the human patient with HPS, suggests that all three will most likely reduce protein stability (Fig. S2).

Vps33A Associates with the HOPS Complex via an Interaction with Vps16 Residues 642–736. We sought to identify the molecular basis of Vps33A recruitment to the rest of HOPS. Because we were unable to express human HOPS components other than Vps33A in *E. coli*, the six proteins that comprise mammalian HOPS (Vps11, Vps16, Vps18, Vps33A, Vps39, and Vps41) were produced individually by in vitro transcription/translation tagged with an N-terminal Myc epitope. As shown in Fig. 2*A*, Vps16 was the only HOPS component "pulled down" by bacterially expressed Vps33A-GST.

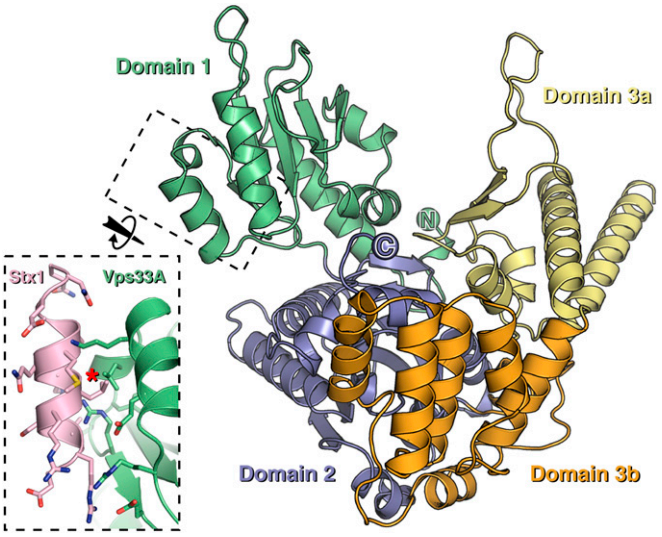

Fig. 1. Human Vps33A is an SM protein but does not bind N-terminal peptides. Human Vps33A is shown as a ribbon, colored by domain. (*Inset*) Model of Vps33A (green) bound to a syntaxin N peptide (Stx1, pink) generated by superposing Vps33A onto the structure of *M. brevicollis* UNC18 in complex with syntaxin 1 (30). Vps33A lacks a pocket (clash marked with a red asterisk) for binding the conserved syntaxin hydrophobic residue (31).

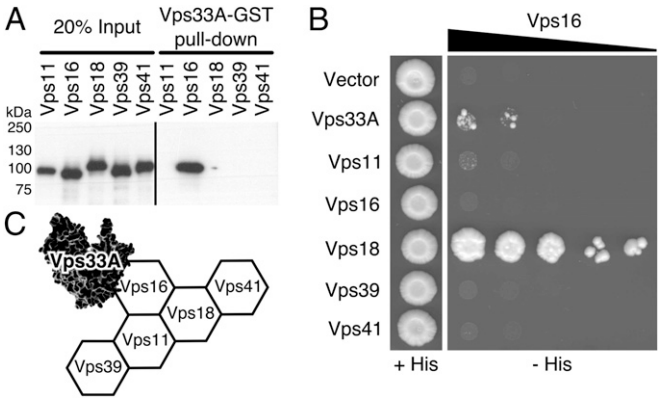

Fig. 2. Human Vps33A binds Vps16. (*A*) Myc-tagged human HOPS components produced by in vitro transcription/translation were incubated with Vps33A-GST and then subjected to GST pull-down and immunoblotting (anti-Myc). (*B*) Yeast two-hybrid interaction of Vps16 (bait) with Vps33A and Vps18 (prey) using the pGBT9/pGAD-C system with selection on plates lacking histidine (–His). The gradient bar indicates fivefold dilutions of the yeast containing both plasmids at each step. (*C*) Schematic representation of the mammalian HOPS complex based on the yeast two-hybrid data shown in Fig. S3. The proposed architecture broadly agrees with that of yeast HOPS (27, 36), with Vps33 at the opposite end of the complex from Vps39.

Yeast two-hybrid interaction studies (Fig. 2*B*) showed that Vps16 "bait" (fused to the Gal4 DNA binding domain) interacted only with Vps33A and Vps18 "prey" (fused to the Gal4 activation domain). Unfortunately, the reciprocal experiment with Vps33A was impossible because fusing Vps33A to the Gal4 DNA binding domain caused autoactivation. Extensive pairwise yeast two-hybrid interaction assays (Fig. S3 and summarized in Fig. 2*C*) showed that Vps33A interacts only with Vps16. Truncation mapping in this yeast two-hybrid system showed that this interaction is mediated by the C-terminal 58-kDa region of Vps16 (Fig. S3).

To determine the minimal region of Vps16 required for binding to Vps33A, a panel of truncated Vps16 constructs was produced by in vitro transcription/translation. Pull-down assays with Vps33A-GST as bait mapped the region of Vps16 necessary for binding to residues 642–736 (Fig. 3 *A* and *B*). This Vps33A binding region of Vps16 was subsequently expressed as a GST fusion in *E. coli* and was used as a bait to pull down recombinant Vps33A successfully, showing that Vps16 residues 642–736 are both necessary and sufficient for binding Vps33A (Fig. 3 *C* and *D*) and that Vps33A is the only HOPS component that binds this region of Vps16 (Fig. 3*C*). The Vps33A homolog Vps33B has recently been shown to interact with a protein that shares significant homology with the C-terminal region of Vps16, termed VIPAR/SPE-39/Vps16B (10, 32–34). Fig. 3*E* shows that, contradictory to the work of Zhu et al. (34) but in agreement with two recent reports (32, 33), Vps33A binds Vps16 but not VIPAR/SPE-39/Vps16B. Similarly, Vps16 residues 642–736 bind Vps33A but not Vps33B (Fig. 3*E*). Yeast two-hybrid experiments also showed that VIPAR/SPE-39/Vps16B interacts with Vps33B but not with Vps33A and that the C-terminal 58-kDa region of Vps16 binds Vps33A but not Vps33B (Fig. S3).

Structure of the Vps33A–Vps16(642–736) Complex. The Vps33A–Vps16(642–736) complex was formed by mixing purified recombinant components, purified by gel filtration, and then crystallized. The structure was solved by molecular replacement, with two molecules of Vps33A being located per asymmetrical unit. Strong difference density not attributable to Vps33A was clearly visible (Fig. S4), and a single molecule of Vps16 was built, spanning Vps16 residues 642–736. The structure of the Vps33A–Vps16(642–736) complex (Fig. 4*A*) with two molecules of Vps33A and one molecule of Vps16 per asymmetrical unit was refined to a resolution of 2.6 Å with residuals R = 0.176 and R_{free} = 0.210

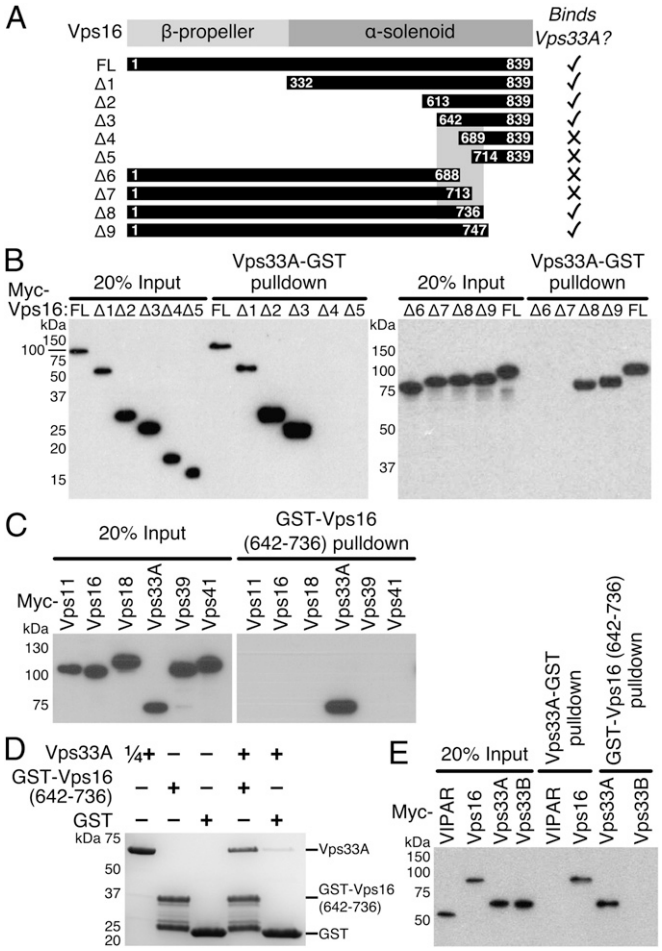

Fig. 3. Residues 642–736 of Vps16 mediate its binding to Vps33A. (*A*) Schematic diagram of Vps16 truncations used in pull-down experiments. The region necessary for binding is shaded gray. (*B*) Full-length (FL) or truncated Myc-Vps16 produced by in vitro transcription/translation was incubated with Vps33A-GST and then subjected to GST pull-down and immunoblotting (anti-Myc). (*C*) Human HOPS components produced by in vitro transcription/translation were incubated with GST-Vps16(642–736) and then subjected to GST pull-down and immunoblotting (anti-Myc). (*D*) Purified Vps33A was incubated with GST or GST-Vps16(642–736) and then subjected to GST pull-down and SDS-PAGE with Coomassie staining. (*E*) Human Vps33A, Vps33B, and Vps16 and VIPAR/SPE-39/Vps16B were produced by in vitro transcription/translation and were incubated with Vps33A-GST or GST-Vps16(642–736) before being subjected to GST pull-down and immunoblotting (anti-Myc).

and excellent stereochemistry, with 98% of residues occupying favored areas of the Ramachandran plot (Table S1).

Residues 642–736 of Vps16 form two long antiparallel helices connected by a loop segment to a bundle of three shorter antiparallel helices (Fig. 4*B*). Although this fold is reminiscent of α-solenoid segments found in proteins involved in membrane trafficking, such as COP-II cage components, the PDBeFold server (35) identifies no significant structural homolog of Vps16.

Size-exclusion chromatography (SEC) with inline multiangle light scattering (MALS) showed purified Vps33A to be monomeric (Fig. 4*C*). SEC-MALS analysis of the Vps33A–Vps16 (642–736) complex showed it to elute from gel filtration with a mass larger than that of a Vps33A monomer but smaller than would be expected for a 1:1 heterodimeric complex (Fig. 4*C*). The observed mass of the Vps33A–Vps16 complex increased when a higher concentration of complex was injected onto the column but did not exceed that expected for a 1:1 heterodimeric complex (Fig. S5). These experiments suggested that Vps16(642–736) binds only a single molecule of Vps33A in solution and that the affinity of this interaction is modest (low micromolar) because the complex dissociates to some degree during SEC.

A single Vps16 molecule contacts four different molecules of Vps33A within the crystal. The most extensive contact is formed between the "inner" concave surface of Vps16 and domain 3b of Vps33A (Fig. 4*A*). This interface buries 1,730 Å^2 of solvent-accessible surface, representing 12.6% of the surface of Vps16 (642–736) and 3.3% of the surface of Vps33A. Analysis of the crystallographic temperature factors supports the identification of this as the relevant interaction interface, because atoms at this interface are better ordered than at the other Vps33A/Vps16 contact surfaces in the crystal (Fig. S6). Site-directed mutagenesis and GST pull-down assays confirmed that this interface mediates the binding of Vps33A to Vps16 in solution (Fig. 5). The mutation A669D or R725E severely disrupts the binding of full-length Vps16 to Vps33A-GST, whereas Vps16 mutations distal from the interaction interface do not disrupt binding (Fig. 5 *A* and *C–E*). Equally, Vps33A with mutation K429D, Y438D, or I441K is not pulled down by GST-Vps16(642–736), whereas mutations far from the interaction interface do not disturb binding (Fig. 5 *B–E*). Further, mutation of a single Vps33A residue at the interaction interface to resemble Vps33B (Y438P) disrupts its ability to bind GST-Vps16(642–736), and the Vps33A-interacting region of Vps16 is not well conserved in VIPAR/SPE-39/Vps16B (Fig. S7).

The most significant difference between Vps16-bound Vps33A and the uncomplexed structure is that the extended helix–turn–helix of domain 3a is well ordered in crystals of the complex and could be modeled. However, this region does not interact with

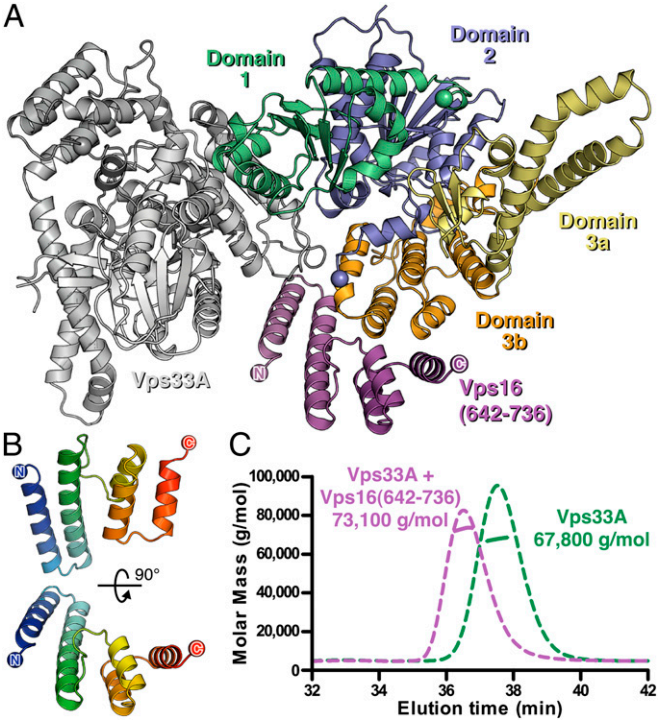

Fig. 4. Structure of Vps33A in complex with Vps16(642–736). (*A*) Cartoon representation of the Vps33A–Vps16(642–736) crystal structure. Vps16 is colored purple, the Vps33A molecule in the asymmetrical unit that makes the most extensive contact with Vps16 is colored by domains (as in Fig. 1), and the other Vps33A molecule is colored gray. (*B*) Vps16 residues 642–736 ramp colored from blue (N terminus) to red (C terminus). (*C*) Static light scattering showing that Vps33A (M_r = 68,979) is monomeric and forms a complex with Vps16(642–736) (M_r = 11,161) that approaches 1:1 stoichiometry in solution.

Vps16 but, instead, contacts the same region from a symmetry-related Vps33A molecule in the crystal. This structural reorganization is therefore unlikely to be relevant for the interaction between Vps33A and Vps16. Residues 531–538 become ordered in one Vps33A molecule in the asymmetrical unit in the presence of Vps16, and residues in this loop contact Vps16 (Fig. 5*C*). However, mutations of L533 or nearby residue F221, or of Vps16 residue A657, do not disrupt complex formation, and we therefore conclude that the ordering of this loop is an artifact of crystallization.

Disrupting the Vps33A–Vps16 Interaction Prevents Recruitment of Vps33A to the HOPS Complex. To investigate whether residues identified as important for the interaction between Vps16 and Vps33A in vitro are required for their interaction in cells, HeLa cell lines were generated that stably expressed N-terminally HA-tagged WT or mutant (A669D or R725E) Vps16. Lysates of these cells were subjected to immunoprecipitation with an anti-HA affinity matrix (Fig. 6*A*). Despite different expression levels of the HA-tagged proteins in the stable cell lines (Fig. 6*A*, *Left*), we were able to immunoprecipitate all HA-tagged Vps16 protein variants (Fig. 6*A*, *Right*) efficiently. Although WT HA-Vps16 co-immunoprecipitated endogenous Vps33A, no interaction between mutant A669D or R725E HA-Vps16 and Vps33A was observed. Although the presence of mutations may cause overall disruption of the HOPS complex, we do not believe that the loss of interaction between HA-Vps16 mutants and Vps33A arises from a complete loss of folding, because both proteins are still competent to co-immunoprecipitate endogenous Vps18, albeit to a lesser extent than WT HA-Vps16, and can thus be successfully incorporated into the HOPS complex (Fig. 6*A*).

We next investigated the residues in Vps33A that were shown to mediate Vps16 binding in vitro (Fig. 5) for a role in cells. We generated stable HeLa cell lines expressing C-terminally Myc-tagged WT or mutant (K428D, Y438D, or I441K) Vps33A, together with WT HA-Vps16. Lysates of these cells were used for immunoprecipitation of WT HA-Vps16 with an anti-HA matrix, and coimmunoprecipitation of overexpressed Vps33A variants was investigated by immunoblotting with an anti-Myc antibody (Fig. 6*B*). Interaction of WT HA-Vps16 was observed with WT Vps33A-Myc and endogenous Vps18. However, none of the mutant Vps33A forms were coimmunoprecipitated with WT HA-Vps16, confirming that the residues K428, Y438, and I441 in Vps33A are required for the interaction with Vps16 in cells. Consistent with our yeast two-hybrid analysis, WT HA-Vps16 retained the ability to immunoprecipitate Vps18, and thus to be incorporated into the HOPS complex in the presence of mutant Vps33A (Fig. 6*B*).

Discussion

The mammalian HOPS complex is a large multisubunit "tethering" complex that binds organelles together and can regulate membrane fusion with late endosomes and lysosomes. Our yeast two-hybrid and GST pull-down studies of isolated human HOPS components show that Vps33A binds only Vps16 and that Vps16 binds Vps33A and Vps18 (Fig. 2), consistent with previous data showing interaction of yeast Vps33 and Vps16 (17, 24, 36, 37). SEC-MALS showed that residues 642–736 of Vps16 form a complex with Vps33A that approaches 1:1 stoichiometry (Fig. 4),

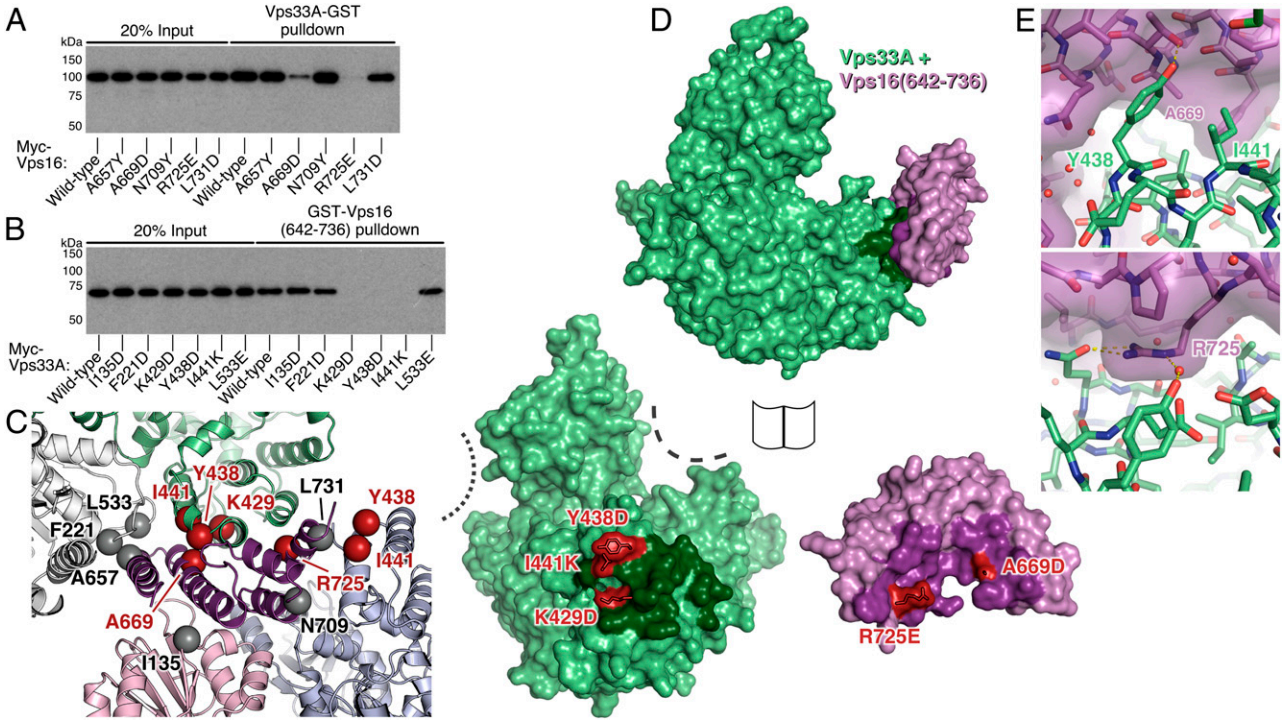

Fig. 5. Site-directed mutagenesis confirms the identity of the Vps16–Vps33A interaction interface. (*A*) Full-length WT or mutant Myc-Vps16 produced by in vitro transcription/translation was incubated with Vps33A-GST and then subjected to GST pull-down and immunoblotting (anti-Myc). (*B*) Full-length WT or mutant Myc-Vps33A produced by in vitro transcription/translation was incubated with GST-Vps16(642–736) and then subjected to GST pull-down and immunoblotting (anti-Myc). (*C*) Cartoon representation of the Vps16 packing environment in Vps33A–Vps16(642–736) crystals. Vps16 is dark purple, and Vps33A molecules that form the most- to least-extensive interfaces with Vps16 in the crystal are shown in green, light blue, light pink, and white, respectively. Residues mutated in *A* and *B* are shown as spheres and colored according to whether they severely disrupt (red) or do not affect (gray) complex formation. (*D*) Open-book representation of Vps33A–Vps16 complex with residues that disrupt the interface highlighted and colored as in *C*. The putative SNARE-binding groove (45) and cleft (46, 47) of Vps33A are marked with dotted and dashed lines, respectively. (*E*) Selected regions of the Vps33A–Vps16 interaction interface are shown as green (Vps33A) and purple (Vps16) sticks with the molecular surface of Vps16 shown as a purple surface.

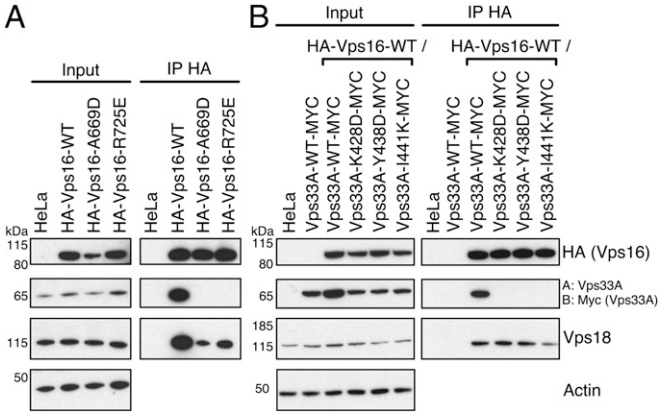

Fig. 6. Mutations in the interaction surface abolish the Vps16–Vps33A association in cells. (*A*) Protein lysates of HeLa cells and HeLa cells stably expressing WT or mutant (A669D or R725E) HA-Vps16 were subjected to immunoprecipitation with anti-HA affinity matrix and immunoblotting. (*B*) Immunoprecipitation with anti-HA matrix from HeLa cells stably expressing WT HA-Vps16, together with WT or mutant (K428D, Y438D, or I441K) Vps33A-Myc. Immunoprecipitation with anti-HA matrix from HeLa cells or HeLa cells stably expressing WT Vps33A-Myc served as a background control. Overexpressed HA-Vps16 and Vps33A-Myc were detected by immunoblotting with anti-HA and anti-Myc antibodies, respectively. Endogenous Vps33A and Vps18 were detected with specific antibodies. Actin served as a loading control.

similar to yeast, where 1:1 stoichiometry of Vps33:Vps16 is observed both in isolated complexes (27) and in intact HOPS (22, 27, 36, 38). Our yeast two-hybrid data on the organization of human HOPS (Fig. S3) are generally consistent with the intramolecular interactions observed in a recent EM reconstruction of the yeast HOPS complex (27), with Vps33A at the opposite end of the complex from Vps39. We therefore propose that the overall architecture of the HOPS complex is likely to be similar in yeast and mammals.

All HOPS complex components except Vps33A are predicted to have a domain organization similar to clathrin, COP-II cage components, and coat nucleoporins, with N-terminal β-propeller domains followed by extended α-solenoids (39–43). Assembly of these coat components is mediated either by interactions between α-solenoid domains (40, 43) or by formation of heteromeric (blade-insertion) β-propellers (40, 42). The majority of interactions observed in our yeast two-hybrid experiments were maintained in the absence of the predicted β-propeller domains (Fig. S3), suggesting that α-solenoid interactions drive assembly of human HOPS.

The structure of Vps33A confirms the prediction that it lacks a pocket for binding the N-terminal peptides of Q_a-SNAREs (31) (Fig. 1). Consistent with this, neither the yeast Q_a-SNARE Vam3 nor its mammalian homologs Stx7 and Stx8 possess an identifiable N peptide (31), and two recent studies have shown yeast Vps33 incapable of binding the N-terminal segment of the Q_a-SNARE Vam3 (23, 24), contradicting a previous report (44). Importantly, both recent studies showed yeast Vps33 capable of binding assembled SNARE complexes (23, 24), and it has therefore been proposed that one function of the other HOPS components is to recruit Vps33, and thus SM protein activity, to the site of SNARE-mediated fusion (24). Although the structure of an SM protein bound to a SNARE complex has yet to be determined, mutagenesis and biochemical studies have identified the SM protein surface groove between domains 1 and 2 (45) and the cleft between domains 1 and 3a (46, 47) as important for the interaction (Fig. S8). The structure of the Vps33A–Vps16 complex shows that the Vps16 binding epitope of Vps33A lies far from proposed SNARE complex interaction sites (Fig. 5 and Fig. S8), consistent with Vps33A binding Vps16 (and thus HOPS) and SNARE complexes simultaneously, although we note that we do not know how the rest of Vps16 is oriented relative to Vps33A in the full HOPS complex.

The Vps33A–Vps16(642–736) structure reveals at atomic resolution how SM proteins bind tethering complex subunits. Vps33A is not the only SM protein that associates with tethering complexes: Yeast Sec1 binds the exocyst complex via exocyst component Sec6 (48), and yeast Sly1 binds the conserved oligomeric Golgi (COG) complex via COG component Cog4 (49). The exocyst and COG complexes are members of the complex associated with tethering containing helical rods (CATCHR) family of multisubunit tethering complexes, which are characterized by their conserved α-helical structures (3). Although high-resolution structures are unavailable for the regions of Cog4 and Sec6 that bind Sly1 and Sec1, it is interesting to note that the segment of Vps16 that mediates its interaction with Vps33A is α-helical (Fig. 4).

The Vps16 binding interface of Vps33A lies almost exclusively on the outer surface of domain 3b (Fig. 4). Previous studies of other SM proteins have implicated this domain not in binding SNAREs or SNARE complexes (45–47) but, rather, in mediating the vesicle tethering/docking step that precedes SNARE complex assembly and vesicle fusion. Mutations of yeast Sec1 domain 3b do not inhibit its ability to bind SNARE complexes but do prevent vesicle docking at the plasma membrane and subsequent SNARE complex formation and cause the same phenotype as observed in yeast mutant *sec6-4*, where exocyst function is disrupted (45). This is consistent with mutations in domain 3b inhibiting its ability to bind the exocyst complex via Sec6 and thereby promoting vesicle docking and SNARE complex formation, although a direct link between Sec6 and Sec1 domain 3b has yet to be identified. Similarly, the interaction between yeast Cog4 and Sly1 is required for co-localization of the SNARE proteins that mediate intra-Golgi and Golgi-to-ER retrograde transport: Disrupting this interaction inhibits retrograde trafficking of cargo (49). Although Sly1 was first characterized as modulating anterograde (ER-to-Golgi) vesicle trafficking (50, 51), a similar retrograde trafficking defect is observed in *sly1-5* mutant yeast bearing a mutation (R452A) in Sly1 domain 3b (52). These observations are consistent with Sly1 domain 3b mediating the interaction with Cog4 in a similar manner to the Vps33A–Vps16 complex. We therefore propose that the structure of Vps33A in complex with Vps16 represents the archetypal interaction between SM proteins and tethering complexes and that the surface of domain 3b is a conserved locus for specific interactions between SM proteins and tethering complexes.

To summarize, we show that the SM protein Vps33A is recruited to the mammalian HOPS complex via an interaction with Vps16 residues 642–736. The structure of the Vps33A–Vps16(642–736) complex allowed us to design single amino acid mutations that disrupt the binding of Vps33A to Vps16, and thus its recruitment to the HOPS complex, both in vitro and in cells. This study provides a structural framework for probing the interactions between SM proteins and tethering complexes.

Materials and Methods

Protein Production and Characterization. Human full-length Vps33A and Vps16 (residues 642–736) with N-terminal (GST-Vps16) or C-terminal (Vps33A-His_{10} and Vps33A-GST) tags were expressed in *E. coli* and purified by affinity, anion exchange (Vps33A only), and SEC using standard protocols. For crystallization, the Vps33A–Vps16 complex was formed by immobilizing GST-Vps16; adding equimolar amounts of Vps33A; liberating the complex with human rhinovirus 3C protease; and then performing SEC, with the Vps33A–Vps16 complex eluting as a single peak.

Structural Analysis. Crystals were grown in sitting drops at 20 °C by mixing protein 1:1 with reservoir solutions as follows: Vps33A-His_{10} (3.2 mg/mL) with 14.3 to 12.8% (wt/vol) PEG 3350 and 143 to 128 mM ammonium acetate, and Vps33A–Vps16 complex (approximately 8.7 mg/mL) with 4% (vol/vol) Tacsimate (pH 6.0; Hampton Research) and 12% (wt/vol) PEG 3350

(Hampton Research). Crystals were cryoprotected with ethylene glycol, and data were recorded at 100 K on Diamond beam line I03 (Vps33A) or I04-1 (Vps33A–Vps16) as detailed in Table S1. The structure of Vps33A was solved by four-wavelength anomalous dispersion analysis of a lead acetate derivative, and the complex structure was solved by molecular replacement using Vps33A as a search model. Final refinement statistics for both structures are shown in Table S1.

Interaction Assays. Details for SEC-MALS, yeast two-hybrid, GST pull-down, and coimmunoprecipitation are provided in *SI Materials and Methods*.

ACKNOWLEDGMENTS. We thank the staff of Diamond Light Source for user support. S.C.G. was supported by the Royal Commission for the Exhibition of 1851 and is currently supported by a Sir Henry Dale Fellowship jointly funded by the Wellcome Trust and the Royal Society (Grant 098406/Z/12/Z). L.W. was supported by European Molecular Biology Organization and Federation of the Societies of Biochemistry and Molecular Biology Long-Term Fellowships. D.J.O. is supported by a Principal Research Fellowship from the Wellcome Trust (Grant 090909/Z/09/Z). The work was funded by the Wellcome Trust (D.J.O.), the Wellcome Trust and the Royal Society (S.C.G.), and UK Medical Research Council Program Grant G0900113 (to J.P.L.). The Cambridge Institute for Medical Research is supported by a Wellcome Trust Strategic Award (Grant 100140). J.E.D. is a Royal Society University Research Fellow.

1. Wickner W (2010) Membrane fusion: Five lipids, four SNAREs, three chaperones, two nucleotides, and a Rab, all dancing in a ring on yeast vacuoles. *Annu Rev Cell Dev Biol* 26:115–136.
2. Bröcker C, Engelbrecht-Vandré S, Ungermann C (2010) Multisubunit tethering complexes and their role in membrane fusion. *Curr Biol* 20(21):R943–R952.
3. Yu IM, Hughson FM (2010) Tethering factors as organizers of intracellular vesicular traffic. *Annu Rev Cell Dev Biol* 26:137–156.
4. Caplan S, Hartnell LM, Aguilar RC, Naslavsky N, Bonifacino JS (2001) Human Vam6p promotes lysosome clustering and fusion in vivo. *J Cell Biol* 154(1):109–122.
5. Kim BY, et al. (2001) Molecular characterization of mammalian homologues of class C Vps proteins that interact with syntaxin-7. *J Biol Chem* 276(31):29393–29402.
6. Poupon V, Stewart A, Gray SR, Piper RC, Luzio JP (2003) The role of mVps18p in clustering, fusion, and intracellular localization of late endocytic organelles. *Mol Biol Cell* 14(10):4015–4027.
7. Seals DF, Eitzen G, Margolis N, Wickner WT, Price A (2000) A Ypt/Rab effector complex containing the Sec1 homolog Vps33p is required for homotypic vacuole fusion. *Proc Natl Acad Sci USA* 97(17):9402–9407.
8. Rink J, Ghigo E, Kalaidzidis Y, Zerial M (2005) Rab conversion as a mechanism of progression from early to late endosomes. *Cell* 122(5):735–749.
9. Pols MS, ten Brink C, Gosavi P, Oorschot V, Klumperman J (2013) The HOPS proteins hVps41 and hVps39 are required for homotypic and heterotypic late endosome fusion. *Traffic* 14(2):219–232.
10. Pulipparacharuvil S, et al. (2005) Drosophila Vps16A is required for trafficking to lysosomes and biogenesis of pigment granules. *J Cell Sci* 118(Pt 16):3663–3673.
11. Liang C, et al. (2008) Beclin1-binding UVRAG targets the class C Vps complex to coordinate autophagosome maturation and endocytic trafficking. *Nat Cell Biol* 10(7):776–787.
12. Koumandou VL, Dacks JB, Coulson RM, Field MC (2007) Control systems for membrane fusion in the ancestral eukaryote; evolution of tethering complexes and SM proteins. *BMC Evol Biol* 7:29.
13. Akbar MA, Ray S, Krämer H (2009) The SM protein Car/Vps33A regulates SNARE-mediated trafficking to lysosomes and lysosome-related organelles. *Mol Biol Cell* 20(6):1705–1714.
14. Suzuki T, et al. (2003) The mouse organellar biogenesis mutant buff results from a mutation in Vps33a, a homologue of yeast vps33 and Drosophila carnation. *Proc Natl Acad Sci USA* 100(3):1146–1150.
15. Wei ML (2006) Hermansky-Pudlak syndrome: A disease of protein trafficking and organelle function. *Pigment Cell Res* 19(1):19–42.
16. Gissen P, et al. (2004) Mutations in VPS33B, encoding a regulator of SNARE-dependent membrane fusion, cause arthrogryposis-renal dysfunction-cholestasis (ARC) syndrome. *Nat Genet* 36(4):400–404.
17. Rieder SE, Emr SD (1997) A novel RING finger protein complex essential for a late step in protein transport to the yeast vacuole. *Mol Biol Cell* 8(11):2307–2327.
18. Südhof TC, Rothman JE (2009) Membrane fusion: Grappling with SNARE and SM proteins. *Science* 323(5913):474–477.
19. Carr CM, Rizo J (2010) At the junction of SNARE and SM protein function. *Curr Opin Cell Biol* 22(4):488–495.
20. Rathore SS, et al. (2010) Syntaxin N-terminal peptide motif is an initiation factor for the assembly of the SNARE-Sec1/Munc18 membrane fusion complex. *Proc Natl Acad Sci USA* 107(52):22399–22406.
21. Hu SH, et al. (2011) Possible roles for Munc18-1 domain 3a and Syntaxin1 N-peptide and C-terminal anchor in SNARE complex formation. *Proc Natl Acad Sci USA* 108(3):1040–1045.
22. Stroupe C, Collins KM, Fratti RA, Wickner W (2006) Purification of active HOPS complex reveals its affinities for phosphoinositides and the SNARE Vam7p. *EMBO J* 25(8):1579–1589.
23. Krämer L, Ungermann C (2011) HOPS drives vacuole fusion by binding the vacuolar SNARE complex and the Vam7 PX domain via two distinct sites. *Mol Biol Cell* 22(14):2601–2611.
24. Lobingier BT, Merz AJ (2012) Sec1/Munc18 protein Vps33 binds to SNARE domains and the quaternary SNARE complex. *Mol Biol Cell* 23(23):4611–4622.
25. Stroupe C, Hickey CM, Mima J, Burfeind AS, Wickner W (2009) Minimal membrane docking requirements revealed by reconstitution of Rab GTPase-dependent membrane fusion from purified components. *Proc Natl Acad Sci USA* 106(42):17626–17633.
26. Starai VJ, Hickey CM, Wickner W (2008) HOPS proofreads the trans-SNARE complex for yeast vacuole fusion. *Mol Biol Cell* 19(6):2500–2508.
27. Bröcker C, et al. (2012) Molecular architecture of the multisubunit homotypic fusion and vacuole protein sorting (HOPS) tethering complex. *Proc Natl Acad Sci USA* 109(6):1991–1996.
28. Bracher A, Weissenhorn W (2001) Crystal structures of neuronal squid Sec1 implicate inter-domain hinge movement in the release of t-SNAREs. *J Mol Biol* 306(1):7–13.
29. Misura KM, Scheller RH, Weis WI (2000) Three-dimensional structure of the neuronal-Sec1-syntaxin 1a complex. *Nature* 404(6776):355–362.
30. Burkhardt P, et al. (2011) Primordial neurosecretory apparatus identified in the choanoflagellate Monosiga brevicollis. *Proc Natl Acad Sci USA* 108(37):15264–15269.
31. Hu SH, Latham CF, Gee CL, James DE, Martin JL (2007) Structure of the Munc18c/Syntaxin4 N-peptide complex defines universal features of the N-peptide binding mode of Sec1/Munc18 proteins. *Proc Natl Acad Sci USA* 104(21):8773–8778.
32. Urban D, et al. (2012) The VPS33B-binding protein VPS16B is required in megakaryocyte and platelet α-granule biogenesis. *Blood* 120(25):5032–5040.
33. Cullinane AR, et al. (2010) Mutations in VIPAR cause an arthrogryposis, renal dysfunction and cholestasis syndrome phenotype with defects in epithelial polarization. *Nat Genet* 42(4):303–312.
34. Zhu GD, et al. (2009) SPE-39 family proteins interact with the HOPS complex and function in lysosomal delivery. *Mol Biol Cell* 20(4):1223–1240.
35. Krissinel E, Henrick K (2004) Secondary-structure matching (SSM), a new tool for fast protein structure alignment in three dimensions. *Acta Crystallogr D Biol Crystallogr* 60(Pt 12 Pt 1):2256–2268.
36. Ostrowicz CW, et al. (2010) Defined subunit arrangement and rab interactions are required for functionality of the HOPS tethering complex. *Traffic* 11(10):1334–1346.
37. Plemel RL, et al. (2011) Subunit organization and Rab interactions of Vps-C protein complexes that control endolysosomal membrane traffic. *Mol Biol Cell* 22(8):1353–1363.
38. Angers CG, Merz AJ (2009) HOPS interacts with Apl5 at the vacuole membrane and is required for consumption of AP-3 transport vesicles. *Mol Biol Cell* 20(21):4563–4574.
39. Nickerson DP, Brett CL, Merz AJ (2009) Vps-C complexes: Gatekeepers of endolysosomal traffic. *Curr Opin Cell Biol* 21(4):543–551.
40. Hoelz A, Debler EW, Blobel G (2011) The structure of the nuclear pore complex. *Annu Rev Biochem* 80:613–643.
41. Brohawn SG, Leksa NC, Spear ED, Rajashankar KR, Schwartz TU (2008) Structural evidence for common ancestry of the nuclear pore complex and vesicle coats. *Science* 322(5906):1369–1373.
42. Fath S, Mancias JD, Bi X, Goldberg J (2007) Structure and organization of coat proteins in the COPII cage. *Cell* 129(7):1325–1336.
43. Lee C, Goldberg J (2010) Structure of coatomer cage proteins and the relationship among COPI, COPII, and clathrin vesicle coats. *Cell* 142(1):123–132.
44. Pieren M, Schmidt A, Mayer A (2010) The SM protein Vps33 and the t-SNARE H(abc) domain promote fusion pore opening. *Nat Struct Mol Biol* 17(6):710–717.
45. Hashizume K, Cheng YS, Hutton JL, Chiu CH, Carr CM (2009) Yeast Sec1p functions before and after vesicle docking. *Mol Biol Cell* 20(22):4673–4685.
46. Shi L, Kümmel D, Coleman J, Melia TJ, Giraudo CG (2011) Dual roles of Munc18-1 rely on distinct binding modes of the central cavity with Stx1A and SNARE complex. *Mol Biol Cell* 22(21):4150–4160.
47. Xu Y, Su L, Rizo J (2010) Binding of Munc18-1 to synaptobrevin and to the SNARE four-helix bundle. *Biochemistry* 49(8):1568–1576.
48. Morgera F, et al. (2012) Regulation of exocytosis by the exocyst subunit Sec6 and the SM protein Sec1. *Mol Biol Cell* 23(2):337–346.
49. Laufman O, Kedan A, Hong W, Lev S (2009) Direct interaction between the COG complex and the SM protein, Sly1, is required for Golgi SNARE pairing. *EMBO J* 28(14):2006–2017.
50. Dascher C, Ossig R, Gallwitz D, Schmitt HD (1991) Identification and structure of four yeast genes (SLY) that are able to suppress the functional loss of YPT1, a member of the RAS superfamily. *Mol Cell Biol* 11(2):872–885.
51. Ossig R, Dascher C, Trepte HH, Schmitt HD, Gallwitz D (1991) The yeast SLY gene products, suppressors of defects in the essential GTP-binding Ypt1 protein, may act in endoplasmic reticulum-to-Golgi transport. *Mol Cell Biol* 11(6):2980–2993.
52. Li Y, Gallwitz D, Peng R (2005) Structure-based functional analysis reveals a role for the SM protein Sly1p in retrograde transport to the endoplasmic reticulum. *Mol Biol Cell* 16(9):3951–3962.